Research Article | Vol. 28, No. 12 / 8 June 2020 / Optics Express 17809
Optics EXPRESS

Digital power division multiplexed DD-OFDM using fundamental mode transmission in few-mode fiber

SMARANIKA SWAIN, SRIKRISHNA BHASHYAM, RAVINDER D. KOILPILLAI, AND DEEPA VENKITESH*

Department of Electrical Engineering, Indian Institute of Technology Madras, Chennai - 600 036, India
**deepa@ee.iitm.ac.in*

Abstract: We experimentally demonstrate fundamental mode transmission of digital power division multiplexed direct detection - orthogonal frequency division multiplexed (DD-OFDM) signal at 25.3 Gbps in 6.5 GHz bandwidth through a 5.3 km few-mode fiber. We compare the performance of a two-channel digital power division multiplexed (DPDM) signal with DD-OFDM of higher modulation format with the same spectral efficiency in both linear and nonlinear regimes of operation. In the linear regime, the mean bit error rate performance of the two-channel DPDM signal performance is comparable to the DD-OFDM signal with higher-order modulation. In the nonlinear regime, both the constituent signals of the DPDM scheme have similar nonlinear thresholds compared to the DD-OFDM signal with higher-order modulation. DPDM transmission with DD-OFDM over few-mode fiber offers doubling of both split ratio and spectral efficiency over single-mode fibers when used for passive optical networks.

1. Introduction

Direct detection based orthogonal frequency division multiplexing (OFDM) has been extensively investigated for passive optical network (PON) applications as a spectrally efficient technique with low implementation cost [1,2]. Split ratio and optical reach in a short-haul optical link employing direct detection are severely limited by the end-to-end power budget. Large effective mode area fibers have been used for fundamental mode transmission in long-haul links owing to their higher nonlinear threshold [3,4]. Fundamental-mode operation (FMO) in standard multimode fiber (SMMF) has been utilized previously to achieve bandwidth-distance product higher than that achievable using standard single-mode fiber (SSMF) [5,6]. Moreover, the majority of record-breaking experiments of recent years have utilized large mode area fibers [7,8]. The reason behind the success of such demonstrations is the fact that a large core diameter would reduce fiber nonlinearity. However, the bandwidth-distance product does not continue to scale linearly with an increase in core diameter due to the presence of differential modal group delay (DMGD), thus limiting the application of FMO in SMMF to only short-haul applications. The effect of DMGD in limiting the bandwidth of such systems is exacerbated in the presence of random coupling between the supported modes [9]. It has been shown that the effect of mode coupling in FMO can only be avoided if only a few modes (2-3) are used [3]. Fundamental mode operation using few-mode fiber (FMF) offers a good compromise between single-mode fiber and multimode fiber since they are significantly more resilient to mode coupling compared to traditional MMF and have a higher nonlinear threshold compared to standard SMF while offering comparable performance as SMFs in terms of dispersion and loss [10,11]. FMO in few-mode fibers has been previously used to achieve optical reach as high as 5032 km [11]. In the case of short-haul links employing direct detection, fundamental mode transmission using few-mode fibers can potentially increase the split ratio by launching of comparatively larger power levels without any distortions due to nonlinear effects, intermodal mixing, or mode-dependent loss.

#394073 https://doi.org/10.1364/OE.394073
Journal © 2020 Received 1 Apr 2020; revised 9 May 2020; accepted 12 May 2020; published 29 May 2020

Optics EXPRESS

Non-orthogonal multiple access (NOMA) based on multiplexing multiple OFDM channels is one of the promising radio access techniques proposed for next-generation cellular communication to provide improved spectral efficiency, better throughput, and low latency [12]. Digital power division multiplexing (DPDM) based on the idea of power domain NOMA has been recently reported as a candidate for flexible PON systems, where the signal reaching different optical network units experience different path losses [13–15]. In DPDM, N independent OFDM signals are combined in the digital domain at specific power ratios using superposition coding before the modulation of the optical carrier. Hence, by appropriate optimization of power division ratios, DPDM is expected to serve as a cost-effective technique to ensure a comparable quality of service for both weak and strong channels in case of links with different known path losses. In the recent past, DPDM was reported as a possible technique to explore "power" as a degree of freedom for multiplexing data [16–18] for optical communication systems, in addition to the traditionally explored multiplexing schemes such as amplitude, time, frequency, phase, and space. In case of amplitude modulation, individual bits are allocated different amplitude (power) levels to generate a modulated signal, whereas, in case of power domain NOMA, N independent OFDM signals with N specific power levels are linearly combined and transmitted. The power domain multiplexed signals can potentially share the same time slot and optical carrier, thus enabling reuse of resources, in addition to improvement in spectral efficiency. Power domain-based NOMA was first demonstrated in this context in [16] by optically combining two DD-OFDM signals with different optical power levels. Digital power division multiplexing was first demonstrated in [17] by combining two DD-OFDM signals digitally, followed by successful transmission of two-channel DPDM using coherent OFDM in the presence of polarization multiplexing for SMF links of length up to 1440 km [18].

It is important to note here that the improvement in spectral efficiency achieved by combining two OFDM signals in the power domain can also be achieved by using a single OFDM signal with a higher modulation format, albeit with a corresponding power/OSNR penalty. For example, spectral efficiency offered by 16QAM-based OFDM is the same as that offered by power domain multiplexing of two OFDM signals utilizing QPSK modulation. However, it is relevant to study the OSNR/power penalty of DPDM compared to 16QAM-based OFDM to achieve the same performance. Digital power division multiplexing as a candidate for spectral efficiency improvement has not been critically evaluated so far by comparing its performance with that of a single channel OFDM signal employing higher order modulation offering the same spectral efficiency. In this work, we compare the performance of 16QAM-based DD-OFDM with that of two-channel DPDM employing QPSK-based DD-OFDM, both of which are expected to offer the same spectral efficiency. In Section 2, we discuss the principle of generation and detection of a two-channel DPDM system used in this work. The experimental set up is discussed in Section 3, followed by the results and discussion in Section 4.

2. Principle of digital power division multiplexing

The block diagram representing the principle of generation of a two-channel DPDM signal [18] is shown in Fig. 1. The QPSK-based DD-OFDM signal $\mathbf{x}(k)$ is generated by digital multiplexing of baseband symbols, $\mathbf{X}_m$, using N point IFFT operation represented as

$$\mathbf{x}(k) = \frac{1}{\sqrt{N}} \sum_{m=0}^{N-1} \mathbf{X}_m exp\left(\frac{j2\pi km}{N}\right); \qquad 0<k<N-1, \tag{1}$$

where N is the total number of subcarriers. In order to generate real $\mathbf{x}(k)$ that is amenable to intensity modulation, we utilize the Hermitian symmetry property of $N-$ point IFFT. Only $\frac{N}{2}$ of total number of subcarriers are filled with data subcarriers and the remaining are generated from their complex conjugates, thus ensuring that the generated $\mathbf{x}(k)$ is real. This is followed

Optics EXPRESS

by insertion of cyclic prefix, parallel to serial conversion and clipping. A second set of OFDM symbols are generated similarly and these two real valued OFDM signals - referred to as $\mathbf{x_1}$ and $\mathbf{x_2}$, are then linearly combined with a specific value of digital power division ratio (*DPDR*), in order to generate the two-channel DPDM signal ($\mathbf{x}_{DPDM}$) represented as

$$\mathbf{x}_{DPDM} = \sqrt{P}\mathbf{x_1} + \sqrt{(1-P)}\mathbf{x_2}, \tag{2}$$

with $DPDR = 10log_{10}\left(\frac{1-P}{P}\right)$. The two baseband time domain signals after power scaling and before combining are shown in Fig. 1. For these demonstrations, P is chosen to be <0.5 such that $\mathbf{x_2}$ and $\mathbf{x_1}$ represent the stronger and weaker channels of the DPDM signal respectively. The two constituent DD-OFDM signals are assigned with non-overlapping training symbols (indicated as TS_1 and TS_2), at the beginning and end of the frame as shown in Fig. 1, to ensure successful channel estimation discussed later in this section.

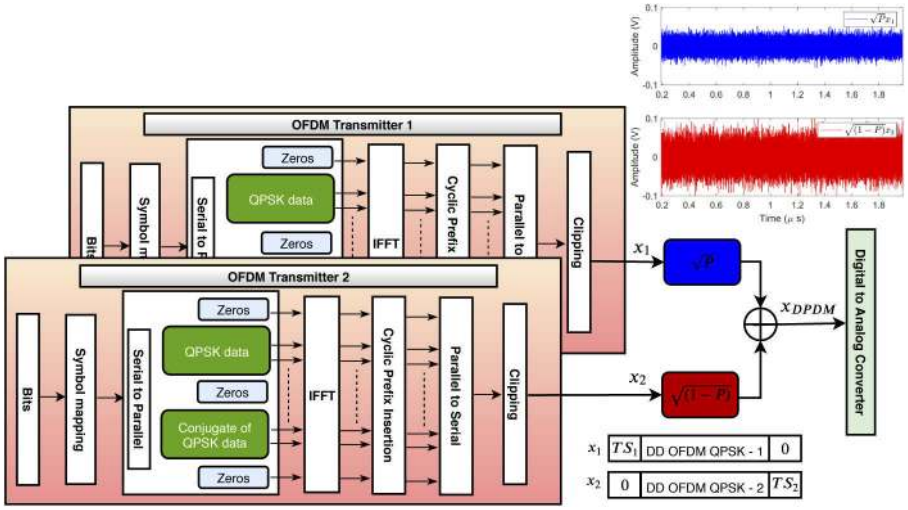

Fig. 1. Block diagram representing generation of DPDM signal (x_{DPDM})

The received time domain signal after propagation through the channel can be written as

$$\mathbf{y_{rec}}(t) = \mathbf{h_1}\sqrt{P}\mathbf{x_1}(t) + \mathbf{h_2}\sqrt{(1-P)}\mathbf{x_2}(t) + \mathbf{n}(t) \tag{3}$$

where $\mathbf{h_1}, \mathbf{h_2}$ are the time domain channel responses experienced by the two individual signals respectively and $\mathbf{n}(t)$ represents the additive white Gaussian noise. Successive interference cancellation (SIC) technique is applied to recover the multiplexed DD-OFDM signals $\mathbf{x_1}(t)$ and $\mathbf{x_2}(t)$. The steps followed to recover the two DD-OFDM signals are shown in Fig. 2. In the pre-processing stage, the serial digital data captured from the analog to digital converter is resampled followed by frame synchronization and serial to parallel conversion. After removal of cyclic prefix and FFT operation, the generated frequency domain signal $\mathbf{Y}_{OFDM-2}$ is passed to the successive interference cancellation stage. First, the frequency domain signal $\mathbf{Y}_{OFDM-2}$ is used to estimate the channel in frequency domain ($\hat{\mathbf{H}}_\mathbf{2}$) and to equalize the stronger signal ($\mathbf{x_2}$). In this step, the signal of lower strength, $\mathbf{x_1}$, is considered as noise. The demodulated stronger signal ($\hat{\mathbf{X}}_\mathbf{2}$) serves as an input to the second step of the SIC technique, where $\hat{\mathbf{X}}_\mathbf{2}$ is first remodulated to generate $\bar{\mathbf{X}}_\mathbf{2}$. The estimated frequency domain channel response $\hat{\mathbf{H}}_\mathbf{2}$ is applied on the remodulated signal. The resulting signal is subtracted from $\mathbf{Y}_{OFDM-2}$ to generate $\mathbf{Y}_{OFDM-1}$ which serves as the input to the second OFDM receiver as shown in Fig. 2 to recover the signal

Optics EXPRESS

with lower strength ($\hat{\mathbf{X}}_\mathbf{1}$). The linear channel estimation and equalization is performed for both the channels by comparing the respective transmitted and received training sequences. The estimated channel response is given by

$$\mathbf{H_i} = \frac{\mathbf{Y}_{OFDM-i}}{TS_i}; i = 1, 2. \tag{4}$$

Bit error rate (BER) is calculated by comparing the equalized and transmitted symbols. The constellations at the output of the channel estimation stages are shown in Fig. 2 for *DPDR* = 5.5 dB, indicating a 16QAM-*like* constellation for the stronger channel ($\mathbf{x_2}$) with higher digital power and a QPSK constellation for the weaker channel ($\mathbf{x_1}$) with lower digital power.

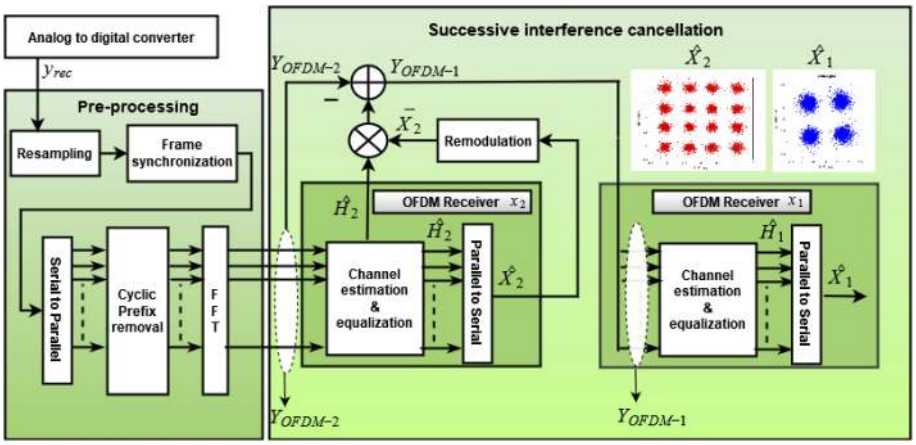

Fig. 2. Block diagram representing recovery of the two baseband OFDM signal ($\mathbf{x_1}$ and $\mathbf{x_2}$) from the received signal y_{rec}

3. Experimental set up

The schematic of the experimental setup used to demonstrate DPDM transmission using intensity modulation and direct detection is shown in Fig. 3. At the transmitter, the baseband QPSK-OFDM signal is generated digitally as described in Section 2. A sampling rate of 15 GSa/s from *PRBS*15 bit sequences is used, with 512 point IFFT, of which 216 subcarriers carry information; and the remaining are their conjugate in order to generate real samples through Hermitian symmetry. The number of subcarriers containing data out of the total number of subcarriers and the position of the empty subcarriers are optimized to achieve minimum BER at a given received power. The total bandwidth used is 6.33 GHz with a subcarrier spacing of 29.3 MHz and data rate of 12.66 Gbps. After parallel to serial conversion, cyclic prefix of length equivalent to 6.25 % of the total frame length is inserted. Two independent OFDM signals ($\mathbf{x_1}$ and$\mathbf{x_2}$) of such identical specifications generated with frame structures shown in Fig. 1 are combined to generate the two-channel DPDM signal offering a net data rate of $\frac{216}{512} \times 15$ GSa/s $\times 2$ (bits/symbol) $\times 2$(DPDM channels) = 25.32 Gbps with a spectral efficiency of 4 bits/sec-Hz. The DPDM signal is clipped to 4 % to minimize the nonlinear effects. The clip ratio (CR) is optimized by observing the EVM as a function of CR for a given bandwidth of operation, in the optical back-to-back condition. The generated signal is upsampled to the sampling rate of the arbitrary waveform generator operating at 60 Gsa/s, and the resulting analog signal is modulated on the optical carrier at 1550 nm using an external intensity modulator (bandwidth : 7.5 GHz) , biased at its quadrature. The modulated optical signal at 1550 nm is amplified and passed through a bandpass filter (bandwidth = 2 nm) to remove the out-of-band noise due to amplified spontaneous emission.

Optics EXPRESS

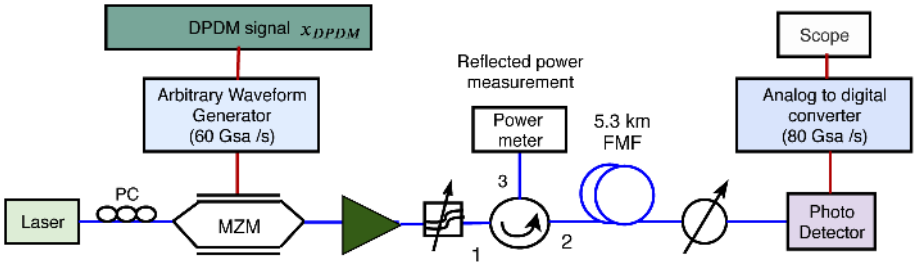

Fig. 3. Schematic of experimental set up for transmission of two-channel DPDM signal through 5.3 km of FMF

The amplified signal is allowed to pass through 5.3 km long FMF that supports LP_{01} and LP_{11} spatial modes. We use a commercially procured graded-index few-mode fiber (GI-FMF), with a trench-assisted cladding to ensure mode confinement of higher-order modes. The parameters of the fiber, as provided by the manufacturer (OFS) are : cladding index of 1.457, the refractive index difference between the peak of core index and cladding index of 7×10^{-3}, numerical aperture of 0.14, and the core diameter of 16 μm. This fiber is found to support the fundamental LP_{01} mode and two higher order degenerate modes- referred to as LP_{11a} and LP_{11b} modes. Using a finite-difference mode solver, we evaluated the effective index difference between the fundamental and higher-order mode for this fiber to be 5×10^{-3} at 1550 nm. This relatively large difference indicates that the intermodal coupling is minimal for short lengths of fibers. The effective area (A_{eff}) of the LP_{01} mode is calcuated as 96 μm^2. The stimulated Brillouin scattering (SBS) threshold of a fiber is found to be directly proportional to A_{eff} [19] and hence the SBS threshold of this fiber is expected to be larger than that of SSMF considering that the A_{eff} of an SSMF is 85 μm^2. Moreover, SBS gain is expected to be highly dependent on the material composition of the fiber [19], the nature of acoustic modes supported by the fiber [20], and hence the Brillouin scattering properties of FMF are expected to be different from that of SMF. A comparison of all the parameters of SSMF and the GI-FMF used in this work is given in Table 1 of the Appendix.

If launching of light from single-mode fiber (which supports only the fundamental mode) to the few-mode fiber is made such that there is a large overlap between the corresponding mode profiles in the two fibers, then light from the fundamental mode of SMF gets coupled into the FMF in its fundamental mode without significant loss. This is achieved by splicing an SMF to the FMF (with the center of the cores aligned), and splicing another SMF at the end to collect only the excited mode. Loss-less coupling from SMFs to large core area fibers is infact commonly reported to be achieved by using standard fusion splicers [4,10,11]. We spliced the two ends of the 5.3 km long FMF to SMFs in a standard fusion splicer (Fujikura 80S) using the core-alignment technique in the automatic mode. Considering the different mode field diameters of the fundamental mode in the SMF and FMF, the theoretically expected splice loss is 0.018 dB [21]. Note that the net splice loss is measured to be 2.1 dB. Considering that the 5.3 km long fiber is constituted by three connectorized FMF spools, and the attenuation in FMF is 0.2 dB/km, we conclude that the contribution to the total loss due to the splicing from SMF to FMF is negligibly small.

The launched power into the FMF is fixed at 0 dBm for the first set of experiments. A circulator is used at the input of the fiber to measure the back-scattered power due to stimulated Brillouin scattering, for the experiments described in Section 4.2. The optical signal, after propagation through FMF, is passed through an attenuator in order to change the power received at the detector. The output of the detector (bandwidth : 9.8 GHz) is received on a real-time oscilloscope of bandwidth 36 GHz and sampling rate of 80 Gsa/s. The captured digital data ($\mathbf{y_{rec}}$) is post processed to recover the two OFDM signals, $\mathbf{x_1}$ and $\mathbf{x_2}$, as discussed in Section 2.

Optics EXPRESS

4. Results and discussion

4.1. Performance analysis of DPDM

Figure 4(a) shows the variation of bit error rate of the two recovered DD-OFDM signals from the digital power division multiplexed signal at two values of received power for different digital power division ratios. The constellations at the output of the two OFDM receivers for $\mathbf{x_1}$ and $\mathbf{x_2}$ are shown as insets in Fig. 4(a) for *DPDR* = 2, 5.5 and 8 dB. As the *DPDR* increases, the performance of the stronger channel ($\mathbf{x_2}$) continuously improves while that of the weaker channel ($\mathbf{x_1}$) degrades after the optimum *DPDR*. The optimized *DPDR* is found to be 5.5 dB for both −6 and −14 dBm received power which confirms that the *DPDR* required for optimum channel performance is independent of the power received at the detector. The *DPDR* of 5.5 dB represents multiplexing of the two QPSK-based DD-OFDM signals at a linear power ratio of 4 : 1 which resembles a 16QAM-*like* constellation, and enables optimum recovery of both channels. The *DPDR* is maintained at 5.5 dB for all further experiments. Note that, this optimized value of DPDR could be specific to the channel used. Figure 4(b) shows variation of BER with received power for both channels of the DPDM signal ($\mathbf{x_1}$ and $\mathbf{x_2}$) and for the constituent QPSK-based DD-OFDM signal for back-to-back condition and for transmission through 5.3 km of FMF.

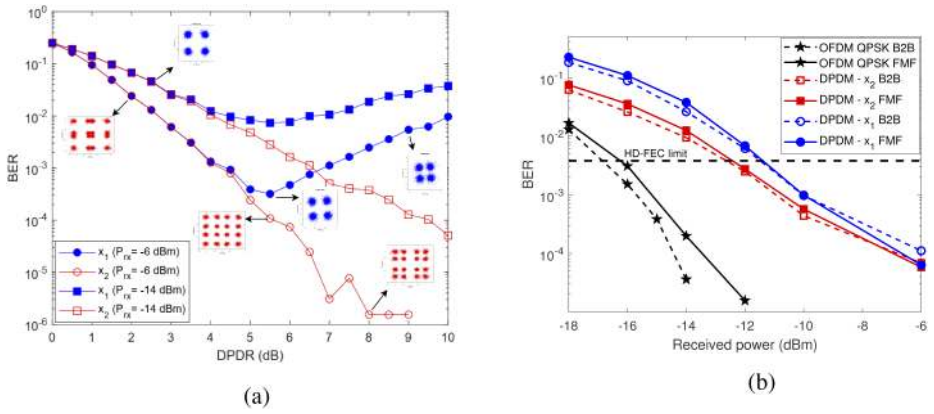

Fig. 4. (a) Variation of BER for $\mathbf{x_1}$ and $\mathbf{x_2}$ for different digital power division ratios and at different levels of received power in back-to-back condition (b) Variation of BER vs received power for the two DPDM channels and for QPSK-based DD-OFDM in back-to-back condition and in the presence of 5.3 km of FMF

The results show successful recovery of both channels of DPDM signal with a 4 dB received power penalty compared to single DD-OFDM signal with QPSK modulation. As expected, the performance of both the channels becomes worse when the received power decreases. The linewidth of the laser is independently characterized to be ≈ 40 KHz. In case of a DD-OFDM signal, laser phase noise contributed by such low linewidth is not expected to degrade the constellations significantly after propagation through 5.3 km fiber [22]. The noise observed in the received constellation is contributed by signal-to-noise ratio at the receiver. Figure 5 shows the variation of mean BER of the two DPDM channels vs received power in back-to-back condition. The performance of QPSK-based DD-OFDM and 16QAM-based DD-OFDM are shown for reference. Note that the spectral efficiency of two-channel DPDM signal is double that of QPSK-based DD-OFDM and is same as 16QAM-based DD-OFDM. It is also clear from Fig. 5 that mean BER performance of the two-channel DPDM signal is comparable to that of 16QAM-based OFDM.

Optics EXPRESS

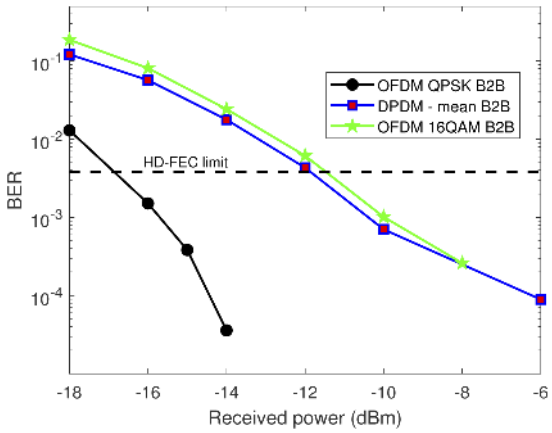

Fig. 5. Variation of mean BER of the two DPDM channels vs received power in back-to-back condition compared with that for QPSK-based OFDM and 16QAM-based OFDM

4.2. *Power budget improvement using FMF*

In order to quantify the improvement in link power budget with the use of FMF, the power launched in to the FMF is gradually increased and the performance is compared by repeating the experiment with same length of SSMF. For the same nonlinear index coefficient, the nonlinear parameter of the FMF is expected to be lower by a factor of 1.25 for the fundamental mode, when compared to SSMF.

The variation of reflected power with increase in input power shown in Fig. 6 indicates an improvement in nonlinear threshold by a factor of 3 dB for FMF. The increase in nonlinear threshold in the communication link enables capacity improvement by transmission of higher-order QAMs. For a short-haul passive optical link, the improvement in nonlinear threshold increases the split ratio. It is clear from Fig. 4(b) that for a desired pre-FEC BER of 3.8×10^{-3}, successful signal recovery at an end user in an access network will require -12 dBm of received power for the stronger channel. Considering nonlinear threshold of 10 dBm and 13 dBm for SMF and FMF respectively, it can be concluded that, the use of FMF can potentially double split ratio for a passive optical network system.

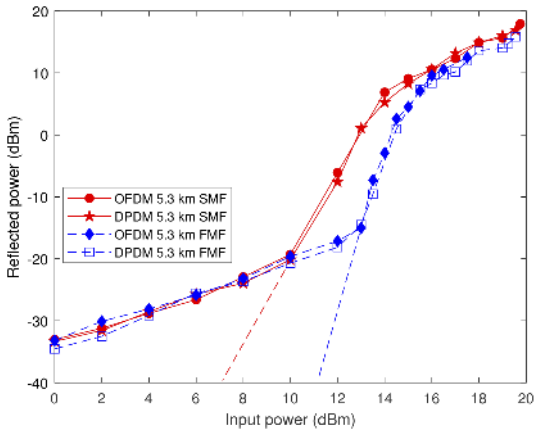

Fig. 6. Variation of reflected power with input power for same length of SMF and FMF (5.3 km).

Optics EXPRESS

The BER performance of QPSK-based DD-OFDM, 16QAM-based DD-OFDM and the two-channel DPDM with increase in input power is shown in Figs. 7(a) and 7(b) for 5.3 km of SMF and FMF respectively. The performance of both two-channel DPDM and 16QAM-based OFDM degrades with input power for 5.3 km of SMF. The recovered constellations corresponding to 5.3 km SMF for 19 dBm of launched power are shown as inset in Fig. 7(a). The captured raw data is distorted because of nonlinear interactions in case of both DPDM and OFDM. However, only OFDM with QPSK modulation is successfully recovered even at power levels >16 dBm. This shows the inherent robustness of QPSK modulation to nonlinear distortions. However, the performance of DPDM degrades under similar conditions. The constellation of the higher strength signal ($\mathbf{x_2}$) resembles 16QAM and hence is more prone to amplitude and phase distortions. Even though the constellation of the lower strength signal ($\mathbf{x_1}$) at the input of OFDM receiver is similar to QPSK, its performance also degrades at such input power levels. This is because, the performance of the weaker channel is not only worse than the stronger DPDM channel ($\mathbf{x_2}$) but is also limited by it. This is expected because in the SIC technique discussed in section II, the stronger channel is remodulated after equalization and demodulation to generate the signal for the second OFDM receiver. Hence, the errors in the detection of the stronger channel directly affects the detection of the weaker channel. This shows that, the digital power division multiplexing scheme has lower nonlinear threshold compared to its constituent OFDM signals in case of single-mode fibers. Additionally, the nonlinear threshold is found to be similar to that of 16QAM-based OFDM which offers same spectral efficiency as the DPDM signal.

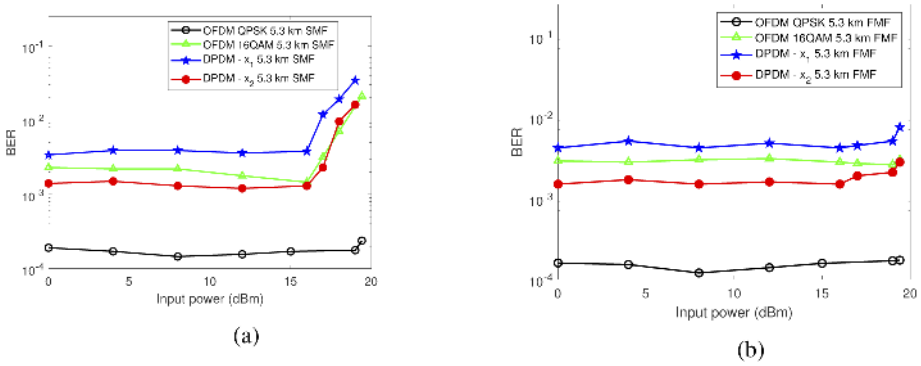

Fig. 7. Variation of BER with input power for same length (5.3 km) of (c) SMF and (d) FMF corresponding to of 5.3 km for QPSK-based DD-OFDM, 16QAM-based DD-OFDM and two-channel DPDM.

Fundamental mode transmission using FMF allows higher launched power levels compared to SMF of same length without any additional changes in network architecture or computational complexity. Figure 7(b) shows variation of BER with input power for 5.3 km of FMF for OFDM, 16QAM OFDM, and the DPDM signal, all of which are successfully recovered for power levels as high as 20 dBm launched in 5.3 km of FMF. The performance of the 16QAM OFDM signal is found to be poorer compared to the stronger DPDM channel ($\mathbf{x_2}$), while it is better compared to the weaker DPDM channel ($\mathbf{x_1}$). The performance improvement due to usage of FMF at higher power levels is found to be same for both DPDM and OFDM.

The demonstrated scheme of direct detection based DPDM transmission using FMF can potentially offer doubling in both spectral efficiency and split ratio in a passive optical network scenario, which is limited by availability of time slot, carrier frequency and received power. Even though the spectral efficiency of two-channel DPDM and OFDM employing 16QAM are identical and the performance of the former is only marginally better, the merit of DPDM lies in the fact that two independent data streams that are accessible to two different users independently, can be

Optics EXPRESS

transmitted using the same optical carrier and time slot. Hence, for short-haul applications that have shared, limited time and spectral resources, the DPDM scheme demonstrated here allows for spectral efficiency improvement using a lower order modulation format by multiplexing signals at specific ratio in the non-orthogonal "power" domain and hence enabling reuse of available time slot and frequency band.

The impact of DPDM is expected to be more significant when the DPDM signal is transmitted through both the modes of the fiber. Intermodal coupling and the differential modal group delay will limit the bandwidth-distance product of such a system. Coherent detection and more complex digital signal processing would be necessary in such a case. DPDM based on coherent OFDM is already reported in [4] for SMF of length >1400 km. Extending this study for multi-mode transmission in few-mode fibers would be a promising approach for scaling capacity and the corresponding study is being taken up independently. However, for short-haul systems, the approach presented in this manuscript using direct detection is attractive for improving spectral efficiency and split ratio.

5. Conclusion

In this paper, we experimentally demonstrate the successful transmission of 25.3 Gbps digital power division multiplexed signal using direct detection over 5.3 km of few-mode fiber in fundamental mode operation condition for the first time. We critically analyze and compare the performance of a two-channel DPDM signal in both linear and nonlinear regime of operation with that of OFDM modulated with a higher modulation format (16QAM). The performance of the 16QAM-based DD-OFDM signal is found to be poorer compared to the stronger DPDM channel and better compared to the weaker DPDM channel. The mean BER performance of the two-channel DPDM signal is comparable to the performance of 16QAM-based DD-OFDM. We also find that DPDM signal multiplexing two OFDM (QPSK) signal is more prone to nonlinear distortions compared to the constituent OFDM (QPSK) signal in a single-mode fiber. This is because the stronger DPDM channel resembles a higher-order modulation format and hence is more prone to amplitude and phase distortions. The performance of the weaker DPDM channel is always worse compared to the stronger channel because errors in the recovery of the stronger channel directly impacts the recovery of the weaker channel due to the successive interference cancellation technique. However, the nonlinear threshold of two-channel DPDM is found to be similar to an OFDM signal employing 16QAM modulation format. This is because a two-channel DPDM signal resembles a 16QAM constellation and hence experiences similar amplitude and phase distortions. The demonstrated two-channel digital power division multiplexing scheme doubles both power split ratio and spectral efficiency compared to the transmission of its constituent OFDM signal through the same length of fiber. The doubling of spectral efficiency using digital power division multiplexing is achieved with the additional advantage of time and frequency reuse compared to OFDM employing a higher-order modulation. A similar scheme implemented with higher order modes is expected to exploit the mode-dependent channel properties to deliver a better throughput.

Appendix A

The specifications of the GI-FMF used in this work are shown in Table 1 and compared with those of SSMF.

Optics EXPRESS

Table 1. Properties of the GI-FMF used in the experiment compared with SSMF

Parameter	GI-FMF	SSMF
Core diameter (μm)	16	8
Cladding diameter (μm)	125 ± 0.7	125 ± 0.7
Cladding non-circularity	<0.7%	<0.7%
Coating diameter (μm)	242 ± 5	242 ± 5
Numerical aperture	0.14	0.14
Attenuation (α) all modes (dB/km)	<0.22	<0.22
Mode field diameter (μm)	LP_{01} : 11 , LP_{11} : 11	10.3
Effective area (μm^2)	LP_{01} : 96 , LP_{11} : 125	85
Dispersion coefficient ($\frac{ps}{nm-km}$)	LP_{01} : 19.9 , LP_{11} : 20	≤ 17.5
Dispersion slope ($\frac{ps}{nm^2-km}$)	LP_{01} : 0.067 , LP_{11} : 20	≤ 17.5
DMGD (ps/m)	0.06	N.A.

Funding

Ministry of Electronics and Information Technology; Visvesvaraya PhD scheme; Office of the Principal Scientific Advisor to the Govt. of India.

Disclosures

The authors declare no conflicts of interest.

References

1. N. Cvijetic, "OFDM for Next-Generation Optical Access Networks," J. Lightwave Technol. **30**(4), 384–398 (2012).
2. J. M. Senior, P. Kourtessis, M. Milosavljevic, and W. Lim, "OFDMA-PON for future generation metro-access networks," in *Photonics Global Conference (PGC)*, (2012), pp. 1–5.
3. Z. Haas and M. A. Santoro, "A mode-filtering scheme for improvement of the bandwidth-distance product in multimode fiber systems," J. Lightwave Technol. **11**(7), 1125–1131 (1993).
4. D. H. Sim, Y. Takushima, and Y. C. Chung, "High-Speed Multimode Fiber Transmission by Using Mode-Field Matched Center-Launching Technique," J. Lightwave Technol. **27**(8), 1018–1026 (2009).
5. P. Nouchi, P. Sansonetti, S. Landais, G. Barre, C. Brehm, J. Y. Boniort, B. Perrin, J. J. Girard, and J. Augé, "Low-loss single-mode fiber with high nonlinear effective area," in *Optical Fiber Communications Conference*, (Optical Society of America, 1995), p. ThH2.
6. H. T. Hattori and A. Safaai-Jazi, "Fiber designs with significantly reduced nonlinearity for very long distance transmission," Appl. Opt. **37**(15), 3190–3197 (1998).
7. X. Zhou, J. Yu, M.-F. Huang, Y. Shao, T. Wang, L. Nelson, P. Magill, M. Birk, P. I. Borel, D. W. Peckham, and R. Lingle, "64-Tb/s (640×107-Gb/s) PDM-36QAM transmission over 320 km using both pre- and post-transmission digital equalization," in *National Fiber Optic Engineers Conference*, (2010), p. PDPB9.
8. J.-X. Cai, Y. Cai, C. R. Davidson, D. G. Foursa, A. Lucero, O. Sinkin, W. Patterson, A. Pilipetskii, G. Mohs, and N. S. Bergano, "Transmission of 96×100G pre-filtered PDM-RZ-QPSK channels with 300% spectral efficiency over 10,608 km and 400% spectral efficiency over 4,368km," in *Optical Fiber Communication Conference (OFC)*, (2010), p. PDPB10.
9. K. Kitayama, S. Seikai, and N. Uchida, "Impulse response prediction based on experimental mode coupling coefficient in a 10-km long graded-index fiber," IEEE J. Quantum Electron. **16**(3), 356–362 (1980).
10. F. Yaman, N. Bai, B. Zhu, T. Wang, and G. Li, "Long distance transmission in few-mode fibers," Opt. Express **18**(12), 13250–13257 (2010).
11. F. Yaman, N. Bai, Y. K. Huang, M. F. Huang, B. Zhu, T. Wang, and G. Li, "10 x 112gb/s pdm-qpsk transmission over 5032 km in few-mode fibers," Opt. Express **18**(20), 21342–21349 (2010).
12. S. M. R. Islam, N. Avazov, O. A. Dobre, and K. Kwak, "Power-domain non-orthogonal multiple access (NOMA) in 5G systems: Potentials and challenges," IEEE Commun. Surv. Tutorials **19**(2), 721–742 (2017).
13. B. Lin, J. Xu, Z. Ghassemlooy, and X. Tang, "Power-code division non-orthogonal multiple access scheme for next-generation passive optical networks," Opt. Express **27**(24), 35740–35749 (2019).
14. F. Lu, M. Xu, L. Cheng, J. Wang, and G. Chang, "Power-Division Non-Orthogonal Multiple Access (NOMA) in Flexible Optical Access With Synchronized Downlink/Asynchronous Uplink," J. Lightwave Technol. **35**(19), 4145–4152 (2017).

Optics EXPRESS

15. B. Lin, Z. Ghassemlooy, X. Tang, Y. Li, and M. Zhang, "Experimental demonstration of an NOMA-PON with single carrier transmission," Opt. Commun. **396**, 66–70 (2017).
16. Z. Feng, M. Tang, X. Guan, C. Chan, Q. Wu, X. Chen, R. Wang, R. Lin, S. Fu, L. Deng, and D. Liu, "Spectrally overlaid DDO-OFDM transmission enabled by optical power division multiplexing," in *15th International Conference on Optical Communications and Networks (ICOCN)*, (2016), pp. 1–3.
17. Z. Feng, M. Tang, X. Guan, C. C. Chan, Q. Wu, R. Wang, R. Lin, S. Fu, L. Deng, and D. Liu, "Digital domain power division multiplexing ddo-ofdm transmission with successive interference cancellation," in *2016 Conference on Lasers and Electro-Optics (CLEO)*, (2016), pp. 1–2.
18. Q. Wu, Z. Feng, M. Tang, X. Li, M. Luo, H. Zhou, S. Fu, and D. Liu, "Digital domain power division multiplexed dual polarization coherent optical ofdm transmission," Sci. Rep. **8**(1), 15827 (2018).
19. V. I. Kovalev and R. G. Harrison, "Threshold for stimulated brillouin scattering in optical fiber," Opt. Express **15**(26), 17625–17630 (2007).
20. W. Chen, G. Hu, F. Liu, F. Wang, C. Song, X. Li, and Y. Yu, "Threshold for stimulated brillouin scattering in few-mode fibers," Appl. Opt. **58**(15), 4105–4110 (2019).
21. A. Ghatak and K. Thyagarajan, *An Introduction to Fiber Optics* (Cambridge University Press, 1998).
22. Y. N. Ali and Z. Zan, "Laser phase noise tolerance in direct detection optical ofdm transmission using laser linewidth emulator," IEEE Photonics J. **9**(6), 1–14 (2017).